TUDelft

Delft University of Technology

Genome duplication and mutations in ACE2 cause multicellar, fast-sedimenting phenotypes in evolved Saccharomyces cerevisiae

Oud, B; Guadalupe Medina, VG; Nijkamp, K; de Ridder, Dick; Pronk, JT; van Maris, AJA; Daran, JM

Important note
To cite this publication, please use the final published version (if applicable).
Please check the document version above.

PNAS

Genome duplication and mutations in *ACE2* cause multicellular, fast-sedimenting phenotypes in evolved *Saccharomyces cerevisiae*

Bart Oud[a,b], Victor Guadalupe-Medina[a,b], Jurgen F. Nijkamp[b,c], Dick de Ridder[b,c,d], Jack T. Pronk[a,b,d], Antonius J. A. van Maris[a,b], and Jean-Marc Daran[a,b,d,1]

[a]Department of Biotechnology, Delft University of Technology, 2628 BC, Delft, The Netherlands; [b]Kluyver Centre for Genomics of Industrial Fermentation, 2600 GA, Delft, The Netherlands; [c]The Delft Bioinformatics Lab, Department of Intelligent Systems, Delft University of Technology, 2628 CD, Delft, The Netherlands; and [d]Platform Green Synthetic Biology, 2600 GA, Delft, The Netherlands

Laboratory evolution of the yeast *Saccharomyces cerevisiae* in bioreactor batch cultures yielded variants that grow as multicellular, fast-sedimenting clusters. Knowledge of the molecular basis of this phenomenon may contribute to the understanding of natural evolution of multicellularity and to manipulating cell sedimentation in laboratory and industrial applications of *S. cerevisiae*. Multicellular, fast-sedimenting lineages obtained from a haploid *S. cerevisiae* strain in two independent evolution experiments were analyzed by whole genome resequencing. The two evolved cell lines showed different frameshift mutations in a stretch of eight adenosines in *ACE2*, which encodes a transcriptional regulator involved in cell cycle control and mother-daughter cell separation. Introduction of the two *ace2* mutant alleles into the haploid parental strain led to slow-sedimenting cell clusters that consisted of just a few cells, thus representing only a partial reconstruction of the evolved phenotype. In addition to single-nucleotide mutations, a whole-genome duplication event had occurred in both evolved multicellular strains. Construction of a diploid reference strain with two mutant *ace2* alleles led to complete reconstruction of the multicellular-fast sedimenting phenotype. This study shows that whole-genome duplication and a frameshift mutation in *ACE2* are sufficient to generate a fast-sedimenting, multicellular phenotype in *S. cerevisiae*. The nature of the *ace2* mutations and their occurrence in two independent evolution experiments encompassing fewer than 500 generations of selective growth suggest that switching between unicellular and multicellular phenotypes may be relevant for competitiveness of *S. cerevisiae* in natural environments.

whole genome sequencing | reverse engineering

Ease of cultivation and genome analysis, short generation times, and large population sizes have contributed to the popularity of microorganisms as model systems in experimental evolution. In addition to providing insights into evolutionary adaptation mechanisms and strategies, laboratory evolution of microorganisms provides a powerful tool to improve characteristics that are relevant to microbial biotechnology. The latter application of laboratory evolution, known as evolutionary engineering (1) has, for example, contributed to expanding substrate range (2–5), functional implementation of alternative product pathways (6, 7), and increased tolerance to inhibitors (4, 8) in various production organisms (9). Recent advances in DNA sequencing and genetic modification facilitate characterization and reconstruction of the genetic changes that underlie evolved phenotypes obtained in laboratory evolution. This progress contributes to identification of the molecular mechanisms that underlie specific phenotypes and enables experimental testing of hypotheses on evolutionary strategies (10). Laboratory evolution has generated new insights into mutation rates (11, 12), genetic drift (12, 13), epistasis (14), clonal interference (15), and other important aspects of evolution by natural selection (16). In microbial biotechnology,

reverse engineering of evolved phenotypes, known as inverse metabolic engineering (17), has similarly benefited from the availability of these genomic methodologies (18). In this applied research context, knowledge of the genetic basis of an industrially relevant phenotype not only increases understanding, but also enables its reconstruction and improvement in other microbial strains and species (18–20).

In unicellular organisms such as the yeast *Saccharomyces cerevisiae*, laboratory evolution is facilitated by the ease with which single-cell lines can be isolated from evolving cultures. Recently, however, Ratcliff et al. described evolution of multicellularity in *S. cerevisiae* within a single long-term cultivation experiment (21). The multicellular variant, in which daughter cells did not separate from the mother cell on cell division, dominated the population within a few generations when fast sedimentation was selected for in test tubes. Evolution of these multicellular clusters of *S. cerevisiae*, which even showed signs of cellular differentiation, was proposed to be a laboratory model for the origin of multicellularity in eukaryotes (21).

At least 25 occurrences of the shift from unicellular to multicellular life forms have been recognized in the evolution of life on Earth (22–24). It has been proposed that multicellularity can contribute to phenotypes as diverse as stress tolerance (25, 26), affinity for substrates (27), and relief of predatory pressure (28). However, knowledge on the selective pressures resulting in the

> ### Significance
>
> The shift from unicellular to multicellular life forms represents a key innovation step in the evolution of life on Earth. However, knowledge on the evolutionary pressures resulting in the selection of multicellular life forms and the underlying molecular mechanisms is far from complete. Our study provides a complete identification of the specific genetic changes by which the unicellular eukaryote *S. cerevisiae* can acquire a multicellular, fast-sedimenting phenotype. We demonstrated that a minimal evolutionary mechanism encompassed a deregulation of the late step of the cell cycle through mutation in *ACE2* followed by whole genome duplication.

evolution of multicellular life forms and on the underlying molecular mechanisms is far from complete.

Knowledge of the mutations that cause the switch from unicellular to multicellular growth in yeast may contribute to understanding of the events leading to the transition to multicellular lives. Moreover, such knowledge can contribute to a better modulation of biomass sedimentation in laboratory research and industrial application of *S. cerevisiae*. In our research on evolutionary engineering of *S. cerevisiae*, we frequently observed multicellular, fast-sedimenting clusters that, on microscopic examination, resemble the phenotype described by Ratcliff et al. (21). The goal of the present study was to elucidate mutations that are responsible for the generation of multicellular variants. To this end, we monitored the formation of multicellular variants in two independent laboratory evolution experiments with a haploid laboratory strain of *S. cerevisiae*. Subsequently, representative mutants from the two evolution experiments were characterized. Genetic changes identified by whole-genome resequencing were reverse engineered in the unicellular parental strain, enabling the identification of two changes that, together, were sufficient to reproduce the multicellular, fast-sedimenting phenotype.

Results

Selection of Multicellular Clusters in Sequential Bioreactor Batch Cultures.
Where previous reports studied evolution of *S. cerevisiae* in serial shake flask cultures (29–33), we reproducibly observed the occurrence of large multicellular clusters during prolonged anaerobic cultivation of the haploid *S. cerevisiae* strain CEN.PK113-7D (34) in sequential bioreactor batch cultures. The phenotype of these clusters was similar to the "snowflake yeast" previously described by Ratcliff and coworkers (21, 35). The design of the "fill and draw" system used in our bioreactors provided an unintended selective advantage to fast-sedimenting cell lines. The vertical pipe used to empty the bioreactor after each cultivation cycle did not reach the bottom of the vessel. Consequently, fast-sedimenting cells were enriched in the small remaining volume used as inoculum for the next batch cultivation cycle.

To facilitate identification of mutations contributing to the multicellular phenotype (18, 33), two identical independent anaerobic evolution experiments were started on a mixture of 20 g·L^{-1} glucose and 20 g·L^{-1} galactose. Although the specific growth rate on galactose doubled during both evolution experiments (from 0.11 to 0.22 and 0.20 h^{-1}; Fig. 1*A* and Fig. S1*A*) and the length of the batch cultivation cycles decreased by at least 35% (Fig. S1 *H* and *I*), the morphology of *S. cerevisiae* changed dramatically as large, multicellular clusters became dominant in both evolution experiments (Fig. 1 *B–F* and Fig. S1 *B–G*). The sedimentation index, calculated from the time-dependent decrease of the optical density of statically incubated cell suspensions, strongly increased, in parallel with the increasing abundance of multicellular clusters (Fig. 1 *B–F* and Fig. S1 *B–G*). Culture samples taken at the end of the two evolution runs [after 4,200 (~900 generations) or 2,880 h (~500 generations)] showed almost complete sedimentation after 5 min of static incubation (Fig. 1*G*).

In *S. cerevisiae*, reversible aggregation of individual cells into fast-sedimenting clusters can occur via flocculation, which involves a Ca^{2+}-dependent interaction of yeast cell wall proteins and carbohydrates (36). However, the multicellular clusters observed in the evolved cultures could not be reverted to a single-cell morphology by incubation with well-known antiflocculent agents such as EDTA (0.5 M) (37), mannose (38), or protease (trypsin 1,500 units·mL^{-1}) (39). This observation indicated that the phenotype did not result from interaction of unicellular yeasts, but rather from an incomplete cell division (36).

Whole Genome Sequence Analysis of Two Evolved Multicellular Isolates.
To investigate the molecular basis of the evolved multicellular phenotype, fast-sedimenting strains IMS0267 and IMS0386 were
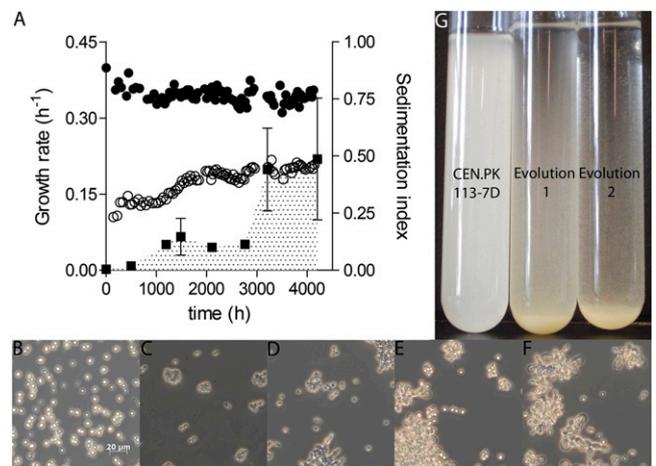

Fig. 1. Sequential batch cultivation in bioreactors on glucose-galactose mixtures results in evolution of multicellular *S. cerevisiae*. (*A*) Maximum specific growth rate (μ_{max}) estimated from CO$_2$ production during glucose consumption in the glucose-galactose batch cultures (●); μ_{max} on galactose estimated from galactose batch cultures (○) in evolution experiment 1. Culture samples were taken at different stages of the evolution experiment, grown to stationary phase in shake flasks containing YP medium with 20 g·L^{-1} glucose, and were left to settle for 30 min in a 1-mL cuvette. Sedimentation indices (■) were calculated as described in *Materials and Methods*. The data represent the average and the mean deviation of duplicate experiments. Microscopic pictures of evolution line 1 after (*B*) 0, (*C*) 1,196 (*D*) 2,105, (*E*) 3,209, and (*F*) 4,200 h of evolution. (*G*) Sedimentation of the reference strain CEN.PK113-7D and a culture sample of evolution lines 1 and 2 after 4,200 and 2,877 h of cultivation, respectively, photographed after 5 min of static incubation.

isolated from evolution experiments 1 and 2, respectively. To verify the genetic stability of the mutations responsible for multicellularity, the evolved strains were grown for at least 50 generations on glucose in shake flask cultures. This test did not result in observable changes in multicellularity or sedimentation behavior, confirming that these phenotypes were independent on the bioreactor context in which they had been evolved and that they were caused by stable mutations. Genomic DNA of strains IMS0267 and IMS0386 was sequenced at high genome coverage (81.6- and 38.5-fold coverage for IMS0267 and IMS0386, respectively) and compared with the reference genome of the parental strain CEN.PK113-7D (34). The high coverage enabled accurate analysis of genomewide copy number variation (CNV) by coassembly (40), as well as identification of single-nucleotide variations (SNV) and indels.

To estimate the ploidy of the evolved strains we de novo coassembled sequence reads of each of the evolved strains with those of the CEN.PK113-7D reference strain. Copy numbers of the assembled contigs were estimated using the Poisson mixture model-based algorithm Magnolya (40). Surprisingly, this analysis revealed that both evolved mutants had undergone a whole-genome duplication event relative to their haploid *MAT*a ancestor CEN.PK113-7D (Fig. 2 *A* and *B*). Both IMS0267 and IMS0386 were for the most part diploid with triplicated genome islands. IMS0267 exhibited triplication of parts of CHRII, XIII, and XVI, whereas IMS0386, besides triplication of parts of CHRIII, VIII, and quadruplication of XIII, had a complete trisomy of CHRII and XI (Fig. 2*A*). Sexual traits of strains IMS0267 and IMS0386 were consistent with a *MAT*a/*MAT*a genotype because these strains were unable to sporulate but were able to mate to a *MAT*α haploid strain (IMI081), with the mating products exhibiting a low efficiency of sporulation.

Mapping of sequence reads of the evolved strains onto the genome sequence of CEN.PK113-7D using the Genome Analysis

Oud et al.
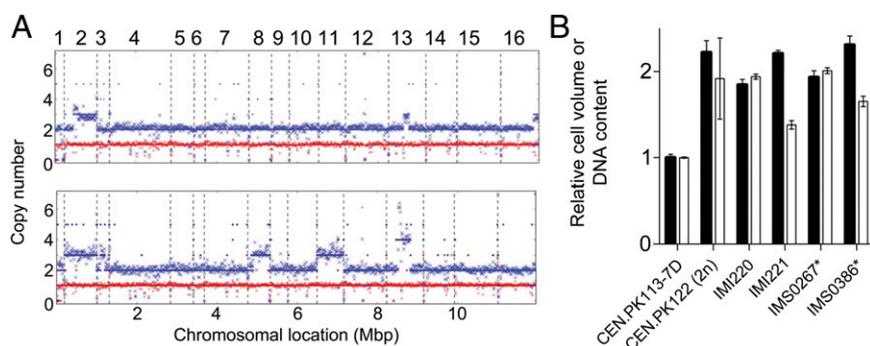
Fig. 2. Ploidy of the evolved mutants IMS0267 and IMS0386. (*A*) Prediction of DNA content in the evolved strains *S. cerevisiae* IMS0267 (*Upper*) and IMS0386 (*Lower*), using the Magnolya algorithm (34). The numbers indicate chromosome position. + (red) indicates the ploidy of the ancestral genome (strain CEN.PK113-7D) and x (blue) indicates the ploidy of the evolved genome. (*B*) Determination of cell size (white bar) and DNA content measurements (black bar) of strains CEN. PK113-7D (*MATa*), CEN.PK122 (*MATa/MATα*), IMS0386, IMS0267, IMI220 (*ACE2/ace2-1-HphNT1*), and IMI221 (*ACE2/ace2-2-HphNT1*) by flow cytometry. Strains IMI220 and IMI221 are unicellular strains derived from IMS0267 and IMS0386 by reintroduction of a WT *ACE2* allele. *For IMS0386 and IMS0267 the analysis was preceded by treatment with *Trichoderma viride* chitinase. Data are presented as average ± mean deviation of duplicate biological replicates.

Toolkit (GATK) software package (41) and assuming a ploidy of 2n revealed 60 mutated positions (SNVs and indels) of which 3 were homozygous and 57 were heterozygous (Table S1). Strikingly, a single gene, *ACE2*, was affected in both strains by two high-probability homozygous indels (Table S1). *ACE2* encodes a transcriptional regulator of, among others, *CTS1*, a gene involved in the final phase of the cell cycle, more specifically required for septum destruction after cytokinesis (42–44). Interestingly, although differently mutated *ACE2* alleles were identified in the evolved isolates, the mutations were found in the same region of *ACE2*: in IMS0267 an adenosine was introduced at position 1,112, whereas in IMS0386 an adenosine was deleted at the same position. The resulting alleles were named *ace2-1* and *ace2-2*. Both mutations caused the introduction of a premature stop codon, at position 1,165 or position 1,114 in IMS0267 and IMS0386, respectively (Fig. S2). Based on its occurrence in both evolved strains and its known role in the yeast cell cycle, we hypothesized that the mutations in *ACE2* contributed to the evolved multicellular phenotype.

ace2-1 and ace2-2 Strains Exhibit Reduced Transcript Levels of Ace2 Targets. The predicted proteins encoded by *ace2-1* and *ace2-2* alleles were 388 and 371 amino acids long instead of 770 amino acids for the original protein (Fig. S2). As a result, the three C2H2-type zinc finger domains and the nuclear localization signal sequence (NLS) located at the C terminus of the Ace2 protein sequence were lost. Conversely, the truncated Ace2 versions retained the nuclear export signal sequence and the interaction domain with Cbk1, a protein kinase involved in the regulation and localization of Ace2. To study the impact of the *ace2* mutations in the evolved multicellular strains, transcription of the previously characterized Ace2 targets *DSE1*/YER124C, *DSE2*/YHR143W, *CTS1*, and *SCW11* (44, 45) was analyzed in the *ace2-1* and *ace2-2* strains by real-time RT-PCR. Expression of all these four Ace2 targets was at least 90% lower in the evolved strains than in the parental strain CEN.PK113-7D (Fig. 3*A*).

Among the targets of Ace2, *CTS1* is of special interest, because it encodes an endo-chitinase required for degradation of the mother-daughter septum (46). Cell wall staining with Calcofluor White, which specifically stains chitin (47), confirmed that within the multicellular clusters, the cells remained attached at the chitin bud neck site (Fig. 3*B*). Consistent with a key role of reduced chitinase expression in the multicellular phenotype, treatment with chitinase led to dispersal of the multicellular clusters into single cells (Fig. 3 *C* and *D*). To test whether reduced expression of *CTS1* is sufficient to cause a multicellular phenotype, we analyzed the phenotype of *cts1Δ* mutants. A homozygous

cts1Δ/cts1Δ strain showed large cell aggregates relative to an isogenic unicellular reference strain (Fig. S3). Sedimentation of the *cts1Δ/cts1Δ* strain was not as fast as in the evolved strains (Fig. S3), which may either reflect differences in strain background or indicate that, in addition to a key role of reduced *CTS1* expression, other factors contribute to the fast-sedimenting phenotype.
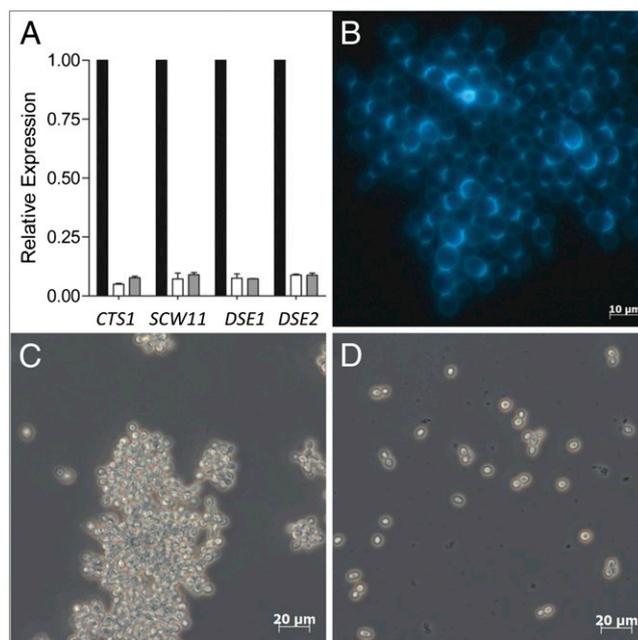
Fig. 3. Effect of mutations in *ACE2* on gene expression and multicellularity. (*A*) Quantification of the expression of characterized Ace2 regulated genes (*CTS1*, *SCW11*, *DSE1*, and *DSE2*) in *S. cerevisiae* strains CEN.PK113-7D (black bar; *ACE2*), IMS0267 (white bar; *ace2-1/ace2-1*), and IMS0386 (gray bar; *ace2-2/ace2-2*). Samples were taken in midexponential phase from a shake flask culture grown on YPD medium. Relative gene expression data represent the expression of *CTS1*, *SCW11*, *DSE1*, and *DSE2* normalized to *ACT1*. The expression ratios were further normalized relative to CEN.PK113-7D. The data represented are average ± mean deviation of duplicate biological replicates. (*B*) Calcofluor White staining of an IMS0267 multicellular cluster. This picture is representative for the entire culture as well as for the two other single-colony isolates obtained from evolved hyper-sedimenting cultures. Microscopic observations of a multicellular cluster of IMS0386 resuspended in 100 mM of potassium phosphate buffer (*C*) before and (*D*) after 7-h incubation with 60 units of chitinase at 25 °C.

Reverse Engineering of ace2 Alleles in Unicellular Strains. To further investigate the importance of the *ace2-1* and *ace2-2* mutations in evolution of multicellular, fast-sedimenting *S. cerevisiae* strains, the WT *ACE2* allele in the haploid ancestor strain CEN.PK113-7D was replaced by either of the two mutant alleles. Neither the introduction of the mutant *ace2* alleles (strains IMI197 and IMK245) nor complete deletion of *ACE2* in CEN.PK113-7D (strain IMK395) resulted in complete reconstruction of the multicellular phenotype of the evolved strains (Fig. 4). The clusters formed by strains IMK395 (*ace2Δ*), IMI197 (*ace2-2-HphNT1*) and IMK245 (*ace2-1-HphNT1*) were much smaller and their sedimentation indices, although significantly higher than that of CEN.PK113-7D, were 10-fold lower than those of the evolved isolates IMS0267 and IMS0386. Conversely, replacement of one of the *ace2-1* or *ace2-2* copies in IMS0267 and IMS0386, respectively, by the WT *ACE2* allele led to a complete reversion of the phenotype to single cells (Fig. 4). This observation confirmed that the *ace2* mutations identified were recessive (IMI220 and IMI221) which could be expected based on the loss of transcriptional activation activity (Fig. 3A).

Estimation of ploidy by flow cytometry analysis of DNA content was not possible with the multicellular evolved strains IMS0267 and IMS0386. We therefore performed the analysis with strains IMI220 (*ace2-1/ACE2*), IMI221 (*ace2-2/ACE2*) and the strains IMS0267 and IMS0386 pretreated with chitinase. Cytometry values confirmed the prediction from sequence coassembly that the evolved strains had undergone a whole genome duplication (Fig. 2 A and B). IMI220 and IMI221 exhibited a 1.9- and a 2.1-fold increase in DNA content, whereas chitinase treated IMS0267 and IMS0386 showed 2.0- and 2.2-fold increased DNA contents, respectively, relative to the haploid reference CEN.PK113-7D (Fig. 2C). To exclude the possibility of transformation-associated selection of unicellular mutants, we confirmed that re-exchanging the *ACE2* WT allele introduced in IMI220 and IMI221 by *ace2-1* [IMW064 (*ace2-1/ace2-1*) and IMW066 (*ace2-1/ace2-2*)] restored formation of large clusters (Fig. S4).

Because the introduction of the *ace2-1* or *ace2-2* alleles in a haploid strain was not sufficient to reconstruct the multicellular phenotype observed in the evolved strains, we investigated the impact of the change in ploidy of the evolved strains on the multicellular phenotype. To this end, the *MATα* strain IMI246
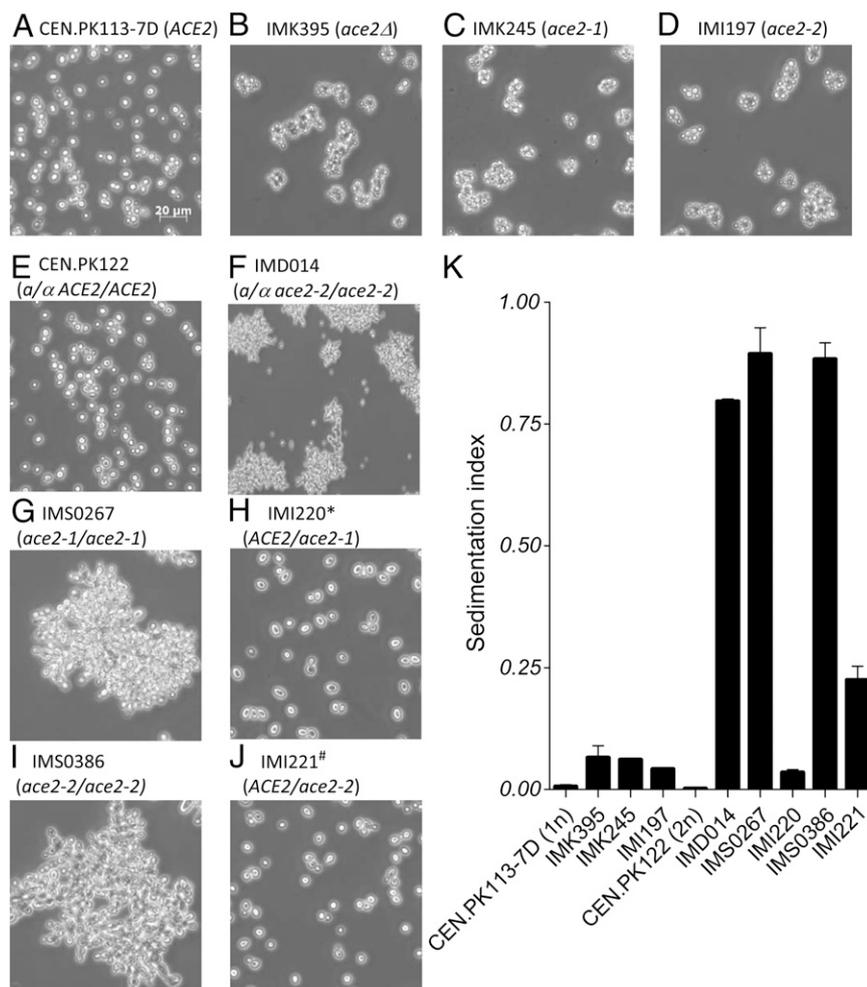
Fig. 4. Reverse engineering of the multicellular phenotype. Cellular morphology of different *S. cerevisiae* strains (*A*) loxP-HphNT1-loxP/ace2-2-loxP-KanMX CEN.PK113-7D (*MATa ACE2*), (*B*) IMK395 (*MATa ace2Δ::loxP-HphNT1-loxP*), (*C*) IMK245 (*MATα ace2-1-loxP-HphNT1-loxP*), (*D*) IMI197 (*ace2-2*), (*E*) CEN.PK122 (*MATa/α ACE2/ACE2*), (*F*) IMD014 (*MATa/α ace2-2-loxP/ ace2-2-loxP*), (*G*) IMS0267 (*ace2-1/ace2-1*), (*H*) IMI220* (*ACE2/ace2-1-loxP-HphNT1-loxP*), (*I*) IMS0386 (*ace2-2/ace2-2*), and (*J*) IMI221# (*ACE2/ace2-2-loxP-HphNT1-loxP*). (*K*) Sedimentation indices (see *Materials and Methods* for definition) of the reference haploid strain CEN.PK113-7D, of the diploid reference CEN.PK122 (*MATa/α*), the evolved multicellular fast-sedimenting strains IMS0267 and IMS0386, and the reverse engineered mutants IMK395, IMK245, IMI197, IMD014, IMI220*, and IMI221#. Data are represented as average ± mean deviation of duplicate biological replicates. *Strains constructed in the evolved IMS0267 background; #strains constructed in the evolved IMS0386 strain background.

(*ace2-2-KanMX*) was constructed by replacing *ACE2* in CEN. PK113-13D and crossed with the *MAT*a strain IMI197 (*ace2-2-HphNT1*). The resulting diploid strain IMD014 (*ace2-2-KanMX/ace2-2-HphNT1*) formed large multicellular clusters (Fig. 4) and exhibited a sedimentation index similar to that of the evolved strains IMS0267 and IMS0386 (Fig. 4). Similarly, the homozygous diploid strains IMD015 (*ace2-1-KanMX/ace2-1-HphNT1*) and IMD017 (*ace2::loxP-HphNT1-loxP/ace2::loxP-KanMX-loxP*), as well as the heterozygous diploid strain IMD016 (*ace2-2-KanMX/ace2-1-HphNT1*) exhibited a multicellular, fast-sedimenting phenotype comparable to that of the two evolved strains IMS0267 and IMS0386 (Fig. S5).

These results demonstrate complete reverse engineering of an evolved multicellular, fast sedimenting phenotype by introduction, in diploid *S. cerevisiae*, of specific recessive mutations in *ACE2* that drastically reduce or eliminate transcriptional activation of Ace2 target genes. Consistent with the ploidy-dependent phenotype of *ace2* null mutants, deletion of the Ace2 target gene *CTS1* in a haploid strain background did not result in the multicellular phenotype observed in diploid *cts1Δ/cts1Δ* strain (Fig. S3).

Discussion

This study provides the first identification of a defined set of genetic changes by which the unicellular eukaryote *S. cerevisiae* can evolve into a multicellular, fast-sedimenting phenotype. Considering the impact of multicellularity in evolution, the molecular events underlying the transformation of unicellular yeast to multicellular clusters were surprisingly simple, requiring only a mutation in a single gene and a whole genome duplication. The recessive characteristic of the *ace2-1* and *ace2-2* mutations strongly suggests that they preceded or even facilitated the origin of the genome duplication event that occurred during laboratory evolution of strains IMS0267 and IMS0386. Although generation of multicellular clusters is easily observable, numerous shake flask–based laboratory evolution studies with *S. cerevisiae* strains, including the strain used in our study, do not report this phenotype (29–33). The fast and reproducible selection of multicellular mutants in the present study was, in all likelihood, a consequence of the design of the effluent-removal system in our bioreactor setups. We thereby inadvertently mimicked the experimental design of Ratcliff and coworkers (21) who intentionally selected for a fast-sedimenting snowflake phenotype by including a biomass settling phase in their serial-batch laboratory evolution experiments.

The accelerated diauxic consumption of glucose-galactose mixtures (Fig. 1A and Fig. S1) by the evolved cultures cannot be completely attributed to the mutations that caused multicellularity (Fig. S6), suggesting that additional mutations contributed to this characteristic. Analysis of several of these mutations, which is outside the scope of this study, was complicated by their heterozygous nature.

The observed ploidy dependency of the phenotype caused by the *ace2* alleles identified in the evolved strains is probably at least partly due to the different bud-site selection preferences of haploid and diploid *S. cerevisiae* strains (48, 49). Haploid cells exhibit axial budding, during which a new bud is formed directly adjacent to the bud scar. Conversely, diploid cells exhibit a polar budding pattern, in which daughter cells bud distally (48). Different bud-site selection strategies will inevitably affect the morphology of multicellular aggregates in mutants with compromised cell division. For example, polar budding should result in less steric hindrance, thereby facilitating generation of larger structures, consistent with the larger size of multicellular clusters in diploid *ace2/ace2* strains. Additionally, ploidy may affect separation of mother and daughter cells even in unicellular strains. Of a set of only 17 *S. cerevisiae* genes whose expression is affected by ploidy (50), two (*CTS1* and *DSE4*, of which only the endo-chitinase–encoding *CTS1* gene is a known Ace2 target) are

associated with mother-daughter cell separation. The strong positive correlation of ploidy and *CTS1* gene expression suggests that, in diploid cells, separation of mother and daughter cells requires more endo-chitinase than in haploids. This assumption would be consistent with the observed stronger phenotype of reduced *CTS1* expression in diploids. The strong ploidy dependence of *ace2* phenotypes underlines the importance of analyzing whole or partial genome duplication in the analysis of evolved strains (51–53). In addition to facilitating the identification of key mutations, research on genome duplication and subsequent further evolution in laboratory experiments may lead to further insight in the evolutionary past of *S. cerevisiae*, in which a whole genome duplication played a pivotal role (54).

Lack of degradation of the chitin septum between the mother and the daughter cells appears to be the predominant mechanism underlying the formation of the multicellular clusters observed in the present study. This mechanism may have played a role in the transition from unicellular fungi to dimorphic and filamentous organisms, because these organisms share a conserved role for chitin in cell wall architecture. Inactivation of the *ACE2* ortholog in the pathogenic yeast *Candida glabrata* led to cell clusters and hypervirulence in a murine model (55, 56). Similarly, *C. albicans* strains with an *ace2Δ/Δ* genotype showed altered separation and morphology and, moreover, resistance to azole antifungal drugs (56). However, outbreaks of hypervirulent and/or antibiotic-resistant mutants of these pathogens have hitherto not been reported.

Although mutations in the endo-chitinase-encoding *CTS1* gene and/or in other components of the regulation of Ace2 and morphogenesis (RAM) pathway can be expected to have similar impacts on sedimentation characteristics, only mutations in *ACE2* were found in two independent evolution experiments. Moreover, the *ace2-1* and *ace2-2* mutations occurred in the same homopolymer of eight adenosine residues (Fig. S2). Poly-(dA: dT) tracts occur frequently in *S. cerevisiae* genome (57, 58), and these regions may participate in the yeast genome evolution by creating mutagenesis hot-spots (57). Poly-(dA:dT) tracts are, however, less abundant in coding regions than in intergenic regions (Table S2), presumably because a resulting evolvability confers a selective disadvantage in most protein-encoding DNA. In contrast, acquisition of a fast-sedimentation phenotype may offer selective advantages in nutrient-rich environments where single cells are easily washed away, such as flowers or fruits subjected to frequent bursts of intensive rainfall. Close inspection of the nucleotide sequences of *Candida ACE2* orthologs, and *S. cerevisiae* genes of the RAM pathway did not reveal homopolymers longer than five residues. In pathogenic *Candida* strains, this might limit the frequency with which hypervirulence occurs as a consequence of loss of function mutations in *ACE2*.

Knowledge of the mutations responsible for a multicellular, fast-sedimenting phenotype in *S. cerevisiae* allows modulation of this property by genetic engineering. The results presented in this study indicate that stable, fast-sedimenting yeast strains for use in cell retention systems can be constructed by inactivation of both copies of *ACE2* in diploid strains. Formation of multicellular clusters, as observed in the evolved strains investigated in this study, does not hinder cell growth. In fact, the evolved strains IMS0267 and IMS0386 showed higher growth rates than their ancestor CEN. PK113-7D in chemically defined medium with glucose and galactose (Fig. 1 and Fig. S1). Additionally, it may be possible to prevent or delay occurrence of multicellular phenotypes in adaptive evolution experiments, where it is not always a desirable feature, by ectopic integration of multiple *ACE2* genes.

Materials and Methods

Strain Maintenance. *S. cerevisiae* strains used in this study (Table 1) were derived from the CEN.PK family (59) and from the BY lineage (60). Strains were maintained on YP medium [demineralized water; 10 g·L^{-1} $\underline{Y}$east extract

(BD Difco); 20 g·L^{-1} Peptone (BD Difco)] with 20 g·L^{-1} glucose (Dextrose) (YPD). Culture stocks were prepared from shake flask cultures, which were incubated at 30 °C and shaken at 200 rpm, by the addition of 20% (vol/vol) glycerol and were stored at −80 °C.

Laboratory Evolution of CEN.PK113-7D and Batch Cultivations. Long-term cultivation in sequential batch reactors was the method used to improve the anaerobic growth characteristics of CEN.PK113-7D in a mixture of 20 g·L^{-1} glucose and 20 g·L^{-1} galactose. Bioreactors were inoculated by adding a shake flask culture that had been grown overnight on synthetic medium (SM) [5 g·L^{-1} (NH$_4$)$_2$SO$_4$, 3 g·L^{-1} KH$_2$PO$_4$, 0.5 g·L^{-1} MgSO$_4$·0.7H$_2$O, trace elements, and vitamins as described in ref. 61], and 20 g·L^{-1} glucose at 30 °C. An alternating batch regime was conducted with every first batch containing 20 g·L^{-1} glucose and 20 g·L^{-1} galactose medium and every second batch containing 20 g·L^{-1} galactose as the sole carbon source in the medium. The cycles on galactose-only medium were included to balance the number of generations of growth on the two sugars (2).

The strains CEN.PK113-7D, CEN.PK122, IMS0267, IMS0386, and IMD014 were compared with respect to fermentation time by batch cultivation in bioreactors. Bioreactors containing SM with 20 g·L^{-1} glucose and 20 g·L^{-1} galactose were inoculated by adding a shake flask culture that had been incubated overnight in synthetic medium and 20 g·L^{-1} galactose at 30 °C. Cultivation was carried out in 2 L laboratory bioreactors (Applikon) with a working volume of 1 L. SM supplemented with 0.01 g·L^{-1} ergosterol and 0.42 g·L^{-1} Tween 80 dissolved in ethanol and trace elements was used as the medium to which either 20 g·L^{-1} glucose and 20 g·L^{-1} galactose or only 20 g·L^{-1} galactose was added. Antifoam Emulsion C (Sigma-Aldrich) was autoclaved separately (120 °C) as a 20% (wt/vol) solution and added to a final concentration of 0.2 g·L^{-1}. Cultures were stirred at 800 rpm, cultures were kept anaerobic by sparging 0.5 L·min^{-1} nitrogen gas (<10 ppm oxygen), and culture pH was kept at 5 by automatically adding 2 M KOH. The bioreactor was equipped with Norprene tubing (Cole Palmer Instrument Company) to minimize oxygen diffusion. The bioreactor was automatically drained when off-gas CO$_2$ levels dropped below 0.05% after the CO$_2$ production peak, leaving 25 (evolution 1) or 5 mL (evolution 2) as inoculum for the next batch. The bioreactor was filled to 1 L using a feed pump controlled by an electric level sensor. For each cycle, the specific growth rate on either glucose or galactose was estimated from the off-gas CO$_2$ production in the exponential phase by fitting an exponential function through the data points. The number of generations was estimated to range from 3.5 to 5 per batch culture based on dry-weight measurements. The culture was regularly checked for purity by plating on lithium-containing agar plates (62) and by microscopy. Culture samples were stored by the addition of 20% (vol/vol) glycerol and kept at −80 °C.

Single Colony Isolation. Representative single colony isolates from the end of both evolution experiments were obtained by biomass samples on YP medium with 20 g·L^{-1} galactose. Single colonies were restreaked twice before inoculating a 15-mL plastic tube containing 1 mL synthetic medium supplemented with vitamins, trace elements, and 20 g·L^{-1} galactose. After incubation for 1 d at 30 °C, these cultures were used to inoculate shake flasks containing 100 mL of the same medium. Fully grown cultures of these shake flasks were stocked. The mutant with the highest sedimentation indices from evolution experiments 1 and 2 were named IMS0267 and IMS0386, respectively.

Calcofluor White Staining. Two hundred microliters of a fully grown shake flask culture on YPD medium was washed thrice in PBS buffer (3.3 mM NaH$_2$PO$_4$, 6.7 mM Na$_2$HPO$_4$, 0.2 mM EDTA, and 130 mM NaCl) and resuspended in 500 μL PBS buffer. One hundred microliters of the resulting suspension was incubated with 10 μL Calcofluor White stain (Calcofluor White M2R 1 g·L^{-1} and Evans Blue 0.5 g·L^{-1}; Fluka). After 15 min, the cell suspension was washed once more. Directly thereafter, phase-contrast and fluorescence microscopy was performed with a Zeiss Imager.D1 microscope equipped with a 40× Plan Neofluor lens and Filter Set 01 (excitation bandpass filter width from 353 to 377 nm, emission long-pass filter from 397 nm, 395-nm beam splitter filter; Carl Zeiss). Images were taken with a Zeiss Axiocam MRc using Axiovision 4.5 software.

Chitinase Assay. One hundred microliters of an overnight shake flask culture on YPD medium was centrifuged and resuspended in either 100 μL 100 mM potassium phosphate buffer (KPB) (pH 6.0) (13.2 mM KH$_2$PO$_4$, 86.8 mM K$_2$HPO$_4$) or 100 μL 100 mM KPB buffer (pH 6.0) with 1 mg ml^{-1} chitinase [chitinase from *Trichoderma viride*, >600 units mg^{-1} (Sigma-Aldrich)].

Sedimentation Assay. To visualize sedimentation in test tubes, yeast cells were harvested from fully grown shake flask cultures on YPD medium, washed twice, and resuspended in SM to a biomass concentration of 2 g dry weight·L^{-1}. After vortexing thoroughly to ensure a homogeneous suspension,

Table 1. Strains used in this study

Strain	Description and genotype	Source
CEN.PK113-7D	*MATa ACE2*	Euroscarf
CEN.PK113-13D	*MATα ura3-52*	Euroscarf
CEN.PK113-16B	*MATα ACE2 leu2-3–112*	Euroscarf
CEN.PK122	*MATa/α ACE2/ACE2*	Euroscarf
IMS0267	*ace2-1/ace2-1*	This study
IMS0386	*ace2-2/ace2-2*	This study
IMK395	*MATa ace2::loxP-HphNT1-loxP*	This study
IMK396	*MATα ura3-52 ace2::loxP-KanMX-loxP*	This study
IMD017	*MATa/α URA3/ura3-52 ace2::loxP-HphNT1-loxP/ ace2::loxP-KanMX-loxP*	This study
IMI196	*MATa ACE2-loxP-HphNT1-loxP*	This study
IMI246	*MATα ura3-52 ace2-2 loxP-KanMX-loxP*	This study
IMI197	*MATa ace2-2-loxP-HphNT1-loxP*	This study
IMK484	*MATa ura3-52 ace2-1-loxP-KanMX-loxP*	This study
IMK245	*MATα ace2-1-loxP-HphNT1-loxP*	This study
IMD014	*MATa/α ura3-52/URA3 ace2-2-loxP-HphNT1-loxP/ace2-2-loxP-KanMX-loxP*	This study
IMD015	*MATa/α ura3-52/URA3 ace2-1-loxP-HphNT1-loxP/ace2-1-loxP-KanMX-loxP*	This study
IMD016	*MATa/α ura3-52/URA3 ace2-2-loxP-HphNT1-loxP/ace2-1-loxP-KanMX-loxP*	This study
IMI220	*ACE2/ace2-1-loxP-HphNT1-loxP**	This study
IMW064	*ace2-1/ace2-1-loxP-KanMX-loxP**	This study
IMI221	*ACE2/ace2-2-loxP-HphNT1-loxP†*	This study
IMW066	*ace2-1/ace2-2-loxP-KanMX-loxP†*	This study
IMI081	*MATα ACE2 leu2-3–112 loxP-HphNT1-loxP*	This study
6947	*MATa his3Δ1 leu2Δ0 met15Δ0 ura3Δ0 cts1::loxP-KanMX-loxP*	Invitrogen
26947	*MATa/α his3Δ1/his3Δ1 leu2Δ0 /leu2Δ0 lys2Δ0/LYS2 cts1::loxP-KanMX-loxP/CTS1*	Invitrogen
36947	*MATa/α his3Δ1/his3Δ1 leu2Δ0 /leu2Δ0 lys2Δ0/LYS2 cts1-loxP/cts1::loxP-KanMX-loxP*	Invitrogen

*Strains constructed in the IMS0267 strain background.
†Strains constructed in the IMS0386 strain background.

Oud et al.

samples were rapidly placed in test tubes, and the clock was immediately started. Photographs were taken after 5 min.

To quantify the rate of sedimentation, shake flask cultures were grown to stationary phase in YPD medium, washed twice, and resuspended in SM to a biomass concentration of 0.42 g dry weight·L^{-1}. The cell suspension was left to settle in a 1-mL cuvette for 30 min while OD_{660} was continuously recorded using a Hitachi U-3010 spectrophotometer (Hitachi High-Technologies Europe). The sedimentation index was defined as the ratio of the decrease of OD_{660} during the 30-min incubation period and the initial OD_{660} value ($\Delta OD_{660}/OD_{660,initial}$).

Whole Genome Sequencing. Genomic DNA from the two evolved strains and CEN.PK113-7D was isolated using the Qiagen 100/G kit (Qiagen). A library of 200-bp genomic fragments was created and paired-end (50-bp reads) sequencing was performed with an Illumina HiSEq 2000 sequencer at Baseclear BV. The individual reads were mapped onto the reference genome of CEN. PK113-7D (34), using the GATK algorithm (41). Single-nucleotide variations, small insertions, and deletions were extracted from the mapping under the assumption that the analyzed genome was diploid. Default settings were used, except that the minimum and maximum read depths were set to 10× and 400×, respectively. To minimize false-positive mutation calls, custom scripts and manual curation were used for further mutation filtering. First, mutation calls that contained ambiguous bases in either reference or mapping consensus were filtered out. Second, only single nucleotide variations with a quality of at least 20 and small insertions and deletions with a quality of at least 60 were kept. Variant quality was defined as the Phred-scaled probability that the mutation call is incorrect (63). Third, mutations with a depth of coverage smaller than 10× were discarded. All variations were manually verified by comparing with raw sequencing data of CEN.PK113-7D.

The Magnolya algorithm (40) was used to analyze copy number variation, using Newbler (454 Life Sciences) for the coassembly. Haploid settings were used for CEN.PK113-7D and diploid settings for the evolved strains to determine their ploidy levels. The raw sequencing data were deposited at the NCBI Sequence Read Archive under BIOproject ID PRJNA193417.

Flow Cytometric Analysis. Cell volumes and the DNA contents of the evolved isolates and a haploid and a diploid reference strain (CEN.PK113-7D and CEN. PK122, respectively) were analyzed by flow cytometry. A culture volume corresponding to 1×10^7 cells·mL^{-1}, determined with a Z2 Coulter Particle Count & Size Analyzer (Beckman Coulter), was centrifuged (5 min, 3,425 × g). The pellet was washed once with phosphate buffer (NaH_2PO_4 3.3 mM, Na_2HPO_4 6.7 mM, NaCl 130 mM, and EDTA 0.2 mM) (64) and resuspended in phosphate buffer. Cells were briefly sonicated (~3 s) in an MSE Soniprep 150 sonicator (150-W output, 7-μm peak-to-peak amplitude; MSE) to prevent cell aggregation. For analysis of evolved strains IMS0267 and IMS0386, cell suspensions were centrifuged and resuspended in 50 mM potassium phosphate buffer (pH 6.0) with 1 mg·mL^{-1} *Trichoderma viride* chitinase (Sigma-Aldrich) and incubated at 30 °C for at least 60 min to disperse cell clusters. After centrifuging (15 min, 1,700 × g), the pellet was washed once in 100 mM potassium phosphate buffer and finally culture samples were resuspended in diluted in IsotonII diluent (Beckman Coulter) to a cell density of ~10^7 mL^{-1}. Cellular DNA was then stained with the Vybrant DyeCycle Orange Stain Kit (Invitrogen) and incubated in the dark for 30 min at 37 °C. Stained and unstained samples were analyzed on a Cell Lab Quanta SC MPL flow cytometer equipped with a 488-nm laser (Beckman Coulter). Quantification of the fluorescence intensity (DNA content) and electronic volume (EV, as a measure for cell volume) was performed by using the free CyFlogic software (version 1.2.1; CyFlo Ltd.).

Quantitative PCR. Transcript levels of Ace2 targets in CEN.PK113-7D, IMS0267, and IMS0386 were determined in duplicate shake flask cultures grown on YPD medium to midexponential phase, when the culture was cooled on ice, and 20 mL of broth was harvested by centrifugation. Total RNA extraction was based on a method described previously (65). Cells were centrifuged and resuspended in one pellet volume of TAE buffer, two pellet volumes of acid phenol-chloroform (5:1, pH 4.5), and 0.1 pellet volume 10% (wt/vol) SDS. The tubes were placed in a water bath at 65 °C for 5 min before being aliquoted in three 1-mL tubes and stored at −80 °C. RNA was extraction as described by Schmitt et al. (66). cDNA was synthesized using the QuantiTect Reverse Transcription Kit (Qiagen). The QuantiTect SYBR Green PCR Kit (Qiagen) was used for quantitative PCR, performed in triplicate and at two dilutions in the Rotor-Gene Q (Qiagen). A primer concentration of 0.5 μM in a total reaction volume of 20 μL was used. All quantitative PCR (qPCR) primers are listed in Table S3. Expression of each transcript relative to the expression in CEN. PK113-7D and normalized to the transcript level of *ACT1* was calculated

using the program REST (Qiagen) by entering take-off and amplification values. A 100% efficient reaction would give an amplification value of 2 for every sample, meaning that the amplicon doubled in every cycle. The actual amplification of the reactions was similar with that obtained using primers for actin *ACT1* (1.65–1.9). Outliers (<1.65) were manually removed. The take-off represents the cycle at which the second derivative is at 20% of the maximum level, indicating the end of the noise and the transition to the exponential phase. The take-off value was calculated for each gene of interest by the Rotor-Gene Q Series Software (Qiagen). Average relative transcript levels were determined from two to four technical replicates. Results presented are averages of at least two biological replicates.

Strain Construction. The protocol described by Gietz and Woods (67) was used to transformation linear DNA fragments into *S. cerevisiae* strains. Transformants were selected on YPD agar plates containing 200 mg·L^{-1} hygromycin B or 200 mg·L^{-1} G418. Transformants were restreaked once before they were confirmed to have the correct integration by PCR (Table S3) on colony material suspended in 0.02 M NaOH and boiled for 10 min. To confirm the presence of the correct allele(s), single read (Sanger) sequencing was performed on selected PCR products by Baseclear BV on an ABI3730XL sequencer (Life Technologies Ltd.).

Disruption of *ACE2* in CEN.PK113-7D was done by integrating the ACE2KO construct, which was amplified by PCR from the plasmid pUG-*hphNT1* (7) with primers ACE2KOf and ACE2KOr. Correct replacement of the *ACE2* gene by the hygromycin B resistance gene was confirmed by PCR with primers sets ACE2fw-Hph NT1 fw, ACE2rv-Hph NT1, and ACE2fw-ACE2rv. The resulting strain was named IMK395 (*ace2Δ::loxP-HphNT1-loxP*).

Introduction of the WT *ACE2* allele (resulting in IMI196), the *ace2-1* allele (resulting in IMK245), and the *ace2-2* allele (resulting in IMI197) into CEN. PK113-7D or introduction of the *ace2-2* allele (resulting in IMI246) and of the *ace2-1* allele (resulting in IMK484) in CEN.PK113-13D was done by cotransformation of two overlapping DNA fragments that recombine with each other and integrate side-by-side into the same chromosomal locus (Fig. S7A). The first fragment contained either the WT *ACE2* allele or an *ace2,* flanked by a unique overlapping sequence with the second fragment. This first construct was obtained by PCR on genomic DNA of CEN.PK113-7D or on genomic DNA of IMS0386 using primers ACE2idF and ACE2tagA. For IMS0267, the first construct was amplified from genomic DNA of IMS0267 using primers ACE2idf and ACE2tagB. The second fragment also contained the unique sequence, together with the hygromycin B or kanamycin resistance gene and a sequence homologous to a sequence 204 bp downstream of *ACE2* (Fig. S7). This second construct was obtained by PCR on the plasmid pUG-*hphNT1* (7) using primers tagApUG and pUGACE2r or by a PCR on pUG6 (68) using primers tagBpUG and pUGACE2r. After integration of the two constructs in the CEN.PK113-7D genome, correct insertion of the constructs was confirmed by PCR using primers pairs ACE2seqf-Hph NT1 rv or ACE2seqf-KanA, ACE2hygidrv-Hph NT1 fw or ACE2hygidrv-KanB, and ACE2seqf-ACE2hygidrv. By sequencing the PCR product obtained from the primer pair ACE2seqf-Hph NT1 rv or ACE2seqf-KanA, the insertion of the correct allele was confirmed using the primer ACE2seqf.

Because the introduction of two genetic elements into the multicellular mutants proved more difficult than in the unicellular ancestor, allele switching in these mutants was done by integrating one complete construct into the *ACE2* locus (Fig. S7B). The construct was obtained by amplifying the complete ACE2-tagA-HphNT1-ACE2 construct from genomic DNA of the appropriate mutants constructed in CEN.PK113-7D by PCR with primers ACE2seqf and ACE2hygidrv. After integration of those constructs in IMS0267 (resulting in IMI220) and IMS0386 (resulting in IMI221), correct insertion of the construct was confirmed by PCR using primer pairs ACE2f-Hph NT1 rv, ACE2TARcheck-Hph NT1 fw, and ACE2f-ACE2TARcheck. By sequencing the PCR product obtained from the primer pair ACE2f-Hph NT1 rv and by sequencing the smaller PCR product from the primer pair ACE2f-ACE2TARcheck using the primer ACE2seqf, presence of the expected alleles was confirmed.

Construction of a diploid *ace2-2/ace2-2* mutant (IMD014) was done by crossing strain IMI197 and strain IMI246 on YPD agar plates. The resulting diploid strain was selected on synthetic agar medium with 200 mg·L^{-1} G418 and hygromycin by restreaking twice on this medium. Correct insertion of the correct alleles was confirmed by sequencing the PCR product obtained from the primer pair ACE2f-Hph NT1 rv and by sequencing the PCR product obtained from the primer pair ACE2f-KanA. Similarly, the strain IMD015 was constructed by crossing IMK484 with IMK245, and the strain IMD016 was constructed by crossing IMI246 with IMK245.

Reintroduction of relevant *ace2* alleles into IMI220 (*ACE2/ace2-1*) and IMI221 (*ACE2/ace2-2*), resulting in strains IMW064 (*ace2-1/ace2-1*) and IMW066 (*ace2-2/ace2-2*), respectively, was done by integrating two

overlapping constructs into the *ACE2* locus, thereby replacing the ACE2-tagA-HphNTI-ACE2 construct (Fig. S7A). The first construct contained an *ace2-1* or *ace2-2* allele, flanked by a unique overlapping sequence with the second construct. The first construct was obtained by PCR on genomic DNA of IMS0267 or IMS0386, using primers ACE2idf and ACE2tagB. The second construct also contained the unique sequence, together with the kanamycin resistance gene and a sequence homologous to a sequence 204 bp downstream of *ACE2*. This second construct was obtained by PCR on the plasmid pUG6 (68) using primers tagBpUG and pUGACE2r. After transformation of the two constructs to the appropriate strain, correct insertion was confirmed by PCR using primer pairs ACE2f-KanA, ACE2TARcheck-KanB, and ACE2f-ACE2TARcheck, as well as by demonstrating resistance to G418 plates but not to hygromycin. Presence of the desired alleles was confirmed by sequencing the PCR product obtained from the primer pair ACE2f-Hph NT1 rv and by sequencing the smaller PCR product from the primer pair ACE2f-ACE2TARcheck using the primer ACE2seqf. Introduction of a hygromycin resistance gene into the *MATα* CEN.PK113-16B strain was done by transforming a genetic construct obtained by PCR from the plasmid pUG-*hphNT1* (7) using primers MTH1markfw and MTH1markrv. The resulting strain was named IMI081 (*ACE2 loxP-HphNT1-loxP*).

Constructs were made by PCR amplification on genomic DNA by using Expand high fidelity Polymerase (Roche) according to the manufacturer's instructions in a Biometra TGradient Thermocycler (Biometra). Isolation of fragments from gel was done with the Zymoclean Gel DNA Recovery kit (Zymo Research). PCR amplification on colony material was done using FastStart Taq DNA Polymerase (Roche) according to the manufacturer's instructions on colony material suspended in 0.02 M NaOH and heated for 10 min at 100 °C.

Mating and Sporulation. Strains IMS0267 and IMS0386 were mated with IMI081 by streaking both strains on YPD plates. After overnight incubation at 30 °C, the strains were streaked over each other. After another 4 h of incubation at 30 °C, diploids were selected by streaking on selective medium (SM medium with 20 g·L^{-1} glucose and 200 mg·L^{-1} hygromycin). Resulting single colonies were restreaked twice on the same medium.

Sporulation was performed by incubating a culture in YP medium supplemented with 10 g·L^{-1} potassium acetate for 2 d at 23 °C. Subsequently, the entire culture was washed twice, resuspended in 20 g·L^{-1} potassium acetate, and incubated for 3–4 d at 23 °C. Spores were segregated on YPD plates using a micromanipulator (Singer Instruments) and incubated at 30 °C.

Homopolymer Distribution. The *S. cerevisiae* reference genome and its annotation (release 64-1-1, February 3, 2011) were downloaded from the *Saccharomyces* Genome Database (www.yeastgenome.org/) (69). A file "domains.tab," containing domains predicted using InterProScan (70), was downloaded from the same site (March 10, 2013). The number of occurrences of dA:dT homopolymers of eight or more residues was counted in the overall genome, in genes (i.e., sequences annotated as gene in the reference genome), in coding sequences within genes, in introns, and in domains. Homopolymers were considered present when all bases fell inside the genomic feature. For each of these features, a Fisher exact test (two-tailed) was then performed under the null hypothesis that the occurrence of homopolymeric stretches is independent of the underlying genomic feature (genes, coding sequences, introns, and domains).

1. Sauer U (2001) Evolutionary engineering of industrially important microbial phenotypes. *Adv Biochem Eng Biotechnol* 73:129–169.
2. Wisselink HW, Toirkens MJ, Wu Q, Pronk JT, van Maris AJA (2009) Novel evolutionary engineering approach for accelerated utilization of glucose, xylose, and arabinose mixtures by engineered *Saccharomyces cerevisiae* strains. *Appl Environ Microbiol* 75(4):907–914.
3. Kuyper M, et al. (2005) Evolutionary engineering of mixed-sugar utilization by a xylose-fermenting *Saccharomyces cerevisiae* strain. *FEMS Yeast Res* 5(10):925–934.
4. Guadalupe Medina V, Almering MJH, van Maris AJA, Pronk JT (2010) Elimination of glycerol production in anaerobic cultures of a *Saccharomyces cerevisiae* strain engineered to use acetic acid as an electron acceptor. *Appl Environ Microbiol* 76(1):190–195.
5. Koppram R, Albers E, Olsson L (2012) Evolutionary engineering strategies to enhance tolerance of xylose utilizing recombinant yeast to inhibitors derived from spruce biomass. *Biotechnol Biofuels* 5(1):32.
6. Zelle RM, Harrison JC, Pronk JT, van Maris AJA (2011) Anaplerotic role for cytosolic malic enzyme in engineered *Saccharomyces cerevisiae* strains. *Appl Environ Microbiol* 77(3):732–738.
7. de Kok S, et al. (2012) Laboratory evolution of new lactate transporter genes in a *jen1* delta mutant of *Saccharomyces cerevisiae* and their identification as *ADY2* alleles by whole-genome resequencing and transcriptome analysis. *FEMS Yeast Res* 12(3):359–374.
8. Adamo GM, Brocca S, Passolunghi S, Salvato B, Lotti M (2012) Laboratory evolution of copper tolerant yeast strains. *Microb Cell Fact* 11:1.
9. Portnoy VA, Bezdan D, Zengler K (2011) Adaptive laboratory evolution—harnessing the power of biology for metabolic engineering. *Curr Opin Biotechnol* 22(4):590–594.
10. Wagner A (2008) Neutralism and selectionism: A network-based reconciliation. *Nat Rev Genet* 9(12):965–974.
11. Loh E, Salk JJ, Loeb LA (2010) Optimization of DNA polymerase mutation rates during bacterial evolution. *Proc Natl Acad Sci USA* 107(3):1154–1159.
12. Elena SF, Lenski RE (2003) Evolution experiments with microorganisms: The dynamics and genetic bases of adaptation. *Nat Rev Genet* 4(6):457–469.
13. Stanek MT, Cooper TF, Lenski RE (2009) Identification and dynamics of a beneficial mutation in a long-term evolution experiment with *Escherichia coli*. *BMC Evol Biol* 9:302.
14. Kvitek DJ, Sherlock G (2011) Reciprocal sign epistasis between frequently experimentally evolved adaptive mutations causes a rugged fitness landscape. *PLoS Genet* 7(4):e1002056.
15. Kao KC, Sherlock G (2008) Molecular characterization of clonal interference during adaptive evolution in asexual populations of *Saccharomyces cerevisiae*. *Nat Genet* 40(12):1499–1504.
16. Conrad TM, Lewis NE, Palsson BO (2011) Microbial laboratory evolution in the era of genome-scale science. *Mol Syst Biol* 7:509.
17. Bailey JE, et al. (1996) Inverse metabolic engineering: A strategy for directed genetic engineering of useful phenotypes. *Biotechnol Bioeng* 52(1):109–121.
18. Oud B, van Maris AJA, Daran JM, Pronk JT (2012) Genome-wide analytical approaches for reverse metabolic engineering of industrially relevant phenotypes in yeast. *FEMS Yeast Res* 12(2):183–196.
19. Bro C, Nielsen J (2004) Impact of 'ome' analyses on inverse metabolic engineering. *Metab Eng* 6(3):204–211.
20. Teusink B, Bachmann H, Molenaar D (2011) Systems biology of lactic acid bacteria: A critical review. *Microb Cell Fact* 10(Suppl 1):S11.
21. Ratcliff WC, Denison RF, Borrello M, Travisano M (2012) Experimental evolution of multicellularity. *Proc Natl Acad Sci USA* 109(5):1595–1600.
22. Bonner JT (1998) The origins of multicellularity. *Integr Biol Issues News Rev* 1(1):27–36.
23. Rokas A (2008) The origins of multicellularity and the early history of the genetic toolkit for animal development. *Annu Rev Genet* 42:235–251.
24. Knoll AH (2011) The multiple origins of complex multicellularity. *Annu Rev Earth Planet Sci* 39:217–239.
25. Weitao T (2009) Multicellularity of a unicellular organism in response to DNA replication stress. *Res Microbiol* 160(1):87–88.
26. Lindén T, Peetre J, Hahn-Hägerdal B (1992) Isolation and characterization of acetic acid-tolerant galactose-fermenting strains of *Saccharomyces cerevisiae* from a spent sulfite liquor fermentation plant. *Appl Environ Microbiol* 58(5):1661–1669.
27. Koschwanez JH, Foster KR, Murray AW (2011) Sucrose utilization in budding yeast as a model for the origin of undifferentiated multicellularity. *PLoS Biol* 9(8):e1001122.
28. Boraas ME, Seale DB, Boxhorn JE (1998) Phagotrophy by a flagellate selects for colonial prey: A possible origin of multicellularity. *Evol Ecol* 12(2):153–164.
29. Jasmin JN, Zeyl C (2012) Life-history evolution and density-dependent growth in experimental populations of yeast. *Evolution* 66(12):3789–3802.
30. Jasmin JN, Zeyl C (2013) Evolution of pleiotropic costs in experimental populations. *J Evol Biol* 26(6):1363–1369.
31. Samani P, Bell G (2010) Adaptation of experimental yeast populations to stressful conditions in relation to population size. *J Evol Biol* 23(4):791–796.
32. Raynes Y, Gazzara MR, Sniegowski PD (2011) Mutator dynamics in sexual and asexual experimental populations of yeast. *BMC Evol Biol* 11:158.
33. Hong KK, Vongsangnak W, Vemuri GN, Nielsen J (2011) Unravelling evolutionary strategies of yeast for improving galactose utilization through integrated systems level analysis. *Proc Natl Acad Sci USA* 108(29):12179–12184.
34. Nijkamp JF, et al. (2012) *De novo* sequencing, assembly and analysis of the genome of the laboratory strain *Saccharomyces cerevisiae* CEN.PK113-7D, a model for modern industrial biotechnology. *Microb Cell Fact* 11:36.
35. Ratcliff WC, Pentz JT, Travisano M (2013) Tempo and mode of multicellular adaptation in experimentally evolved *Saccharomyces cerevisiae*. *Evolution* 67(6):1573–1581.
36. Soares EV (2011) Flocculation in *Saccharomyces cerevisiae*: A review. *J Appl Microbiol* 110(1):1–18.
37. Soares EV, Vroman A (2003) Effect of different starvation conditions on the flocculation of *Saccharomyces cerevisiae*. *J Appl Microbiol* 95(2):325–330.
38. Stratford M (1992) Yeast flocculation: A new perspective. *Adv Microb Physiol* 33:2–71.

39. Stratford M, Assinder S (1991) Yeast flocculation: Flo1 and NewFlo phenotypes and receptor structure. *Yeast* 7(6):559–574.

40. Nijkamp JF, et al. (2012) *De novo* detection of copy number variation by co-assembly. *Bioinformatics* 28(24):3195–3202.

41. McKenna A, et al. (2010) The Genome Analysis Toolkit: A MapReduce framework for analyzing next-generation DNA sequencing data. *Genome Res* 20(9):1297–1303.

42. Voth WP, Olsen AE, Sbia M, Freedman KH, Stillman DJ (2005) *ACE2, CBK1,* and *BUD4* in budding and cell separation. *Eukaryot Cell* 4(6):1018–1028.

43. Saputo S, Chabrier-Rosello Y, Luca FC, Kumar A, Krysan DJ (2012) The RAM network in pathogenic fungi. *Eukaryot Cell* 11(6):708–717.

44. Doolin MT, Johnson AL, Johnston LH, Butler G (2001) Overlapping and distinct roles of the duplicated yeast transcription factors Ace2p and Swi5p. *Mol Microbiol* 40(2): 422–432.

45. Sbia M, et al. (2008) Regulation of the yeast Ace2 transcription factor during the cell cycle. *J Biol Chem* 283(17):11135–11145.

46. Kuranda MJ, Robbins PW (1991) Chitinase is required for cell separation during growth of *Saccharomyces cerevisiae. J Biol Chem* 266(29):19758–19767.

47. Herth W, Schnepf E (1980) The fluorochrome, calcofluor white, binds oriented to structural polysaccharide fibrils. *Protoplasma* 105(1-2):129–133.

48. Casamayor A, Snyder M (2002) Bud-site selection and cell polarity in budding yeast. *Curr Opin Microbiol* 5(2):179–186.

49. Chant J, Pringle JR (1995) Patterns of bud-site selection in the yeast *Saccharomyces cerevisiae. J Cell Biol* 129(3):751–765.

50. Galitski T, Saldanha AJ, Styles CA, Lander ES, Fink GR (1999) Ploidy regulation of gene expression. *Science* 285(5425):251–254.

51. Yona AH, et al. (2012) Chromosomal duplication is a transient evolutionary solution to stress. *Proc Natl Acad Sci USA* 109(51):21010–21015.

52. Chen GB, Rubinstein B, Li R (2012) Whole chromosome aneuploidy: Big mutations drive adaptation by phenotypic leap. *Bioessays* 34(10):893–900.

53. Koszul R, Caburet S, Dujon B, Fischer G (2004) Eucaryotic genome evolution through the spontaneous duplication of large chromosomal segments. *EMBO J* 23(1):234–243.

54. Wolfe KH, Shields DC (1997) Molecular evidence for an ancient duplication of the entire yeast genome. *Nature* 387(6634):708–713.

55. Kamran M, et al. (2004) Inactivation of transcription factor gene *ACE2* in the fungal pathogen *Candida glabrata* results in hypervirulence. *Eukaryot Cell* 3(2):546–552.

56. MacCallum DM, et al. (2006) Different consequences of *ACE2* and *SWI5* gene disruptions for virulence of pathogenic and nonpathogenic yeasts. *Infect Immun* 74(9): 5244–5248.

57. Ma X, et al. (2012) Mutation hot spots in yeast caused by long-range clustering of homopolymeric sequences. *Cell Rep* 1(1):36–42.

58. Dechering KJ, Cuelenaere K, Konings RN, Leunissen JA (1998) Distinct frequency-distributions of homopolymeric DNA tracts in different genomes. *Nucleic Acids Res* 26(17):4056–4062.

59. Entian KD, Kötter P (2007) Yeast genetic strain and plasmid collections. *Method Microbiol* 36:629–666.

60. Brachmann CB, et al. (1998) Designer deletion strains derived from *Saccharomyces cerevisiae* S288C: A useful set of strains and plasmids for PCR-mediated gene disruption and other applications. *Yeast* 14(2):115–132.

61. Verduyn C, Postma E, Scheffers WA, Van Dijken JP (1992) Effect of benzoic acid on metabolic fluxes in yeasts: A continuous-culture study on the regulation of respiration and alcoholic fermentation. *Yeast* 8(7):501–517.

62. Daran-Lapujade P, et al. (2009) An atypical *PMR2* locus is responsible for hypersensitivity to sodium and lithium cations in the laboratory strain *Saccharomyces cerevisiae* CEN.PK113-7D. *FEMS Yeast Res* 9(5):789–792.

63. Ewing B, Green P (1998) Base-calling of automated sequencer traces using phred. II. Error probabilities. *Genome Res* 8(3):186–194.

64. Porro D, Brambilla L, Alberghina L (2003) Glucose metabolism and cell size in continuous cultures of *Saccharomyces cerevisiae. FEMS Microbiol Lett* 229(2):165–171.

65. Daran-Lapujade P, Daran JM, van Maris AJA, de Winde JH, Pronk JT (2009) Chemostat-based micro-array analysis in baker's yeast. *Adv Microb Physiol* 54:257–311.

66. Schmitt ME, Brown TA, Trumpower BL (1990) A rapid and simple method for preparation of RNA from *Saccharomyces cerevisiae. Nucleic Acids Res* 18(10):3091–3092.

67. Gietz RD, Woods RA (2002) Transformation of yeast by lithium acetate/single-stranded carrier DNA/polyethylene glycol method. *Methods Enzymol* 350:87–96.

68. Gueldener U, Heinisch J, Koehler GJ, Voss D, Hegemann JH (2002) A second set of loxP marker cassettes for Cre-mediated multiple gene knockouts in budding yeast. *Nucleic Acids Res* 30(6):e23.

69. Engel SR, Cherry JM (2013) The new modern era of yeast genomics: Community sequencing and the resulting annotation of multiple *Saccharomyces cerevisiae* strains at the Saccharomyces Genome Database. *Database (Oxford)* 2013:bat012.

70. Mulder N, Apweiler R (2007) InterPro and InterProScan: Tools for protein sequence classification and comparison. *Methods Mol Biol* 396:59–70.